Very strong intrinsic flux pinning and vortex avalanches in (Ba,K)Fe$_2$As$_2$ superconducting single crystals

Xiao-Lin Wang,[1,*] S. R. Ghorbani,[1,2] Sung-Ik Lee,[3,†] S. X. Dou,[1] C. T. Lin,[4] T. H. Johansen,[1,5] K.-H. Müller,[6] Z. X. Cheng,[1] G. Peleckis,[1] M. Shabazi,[1] A. J. Qviller,[5] V. V. Yurchenko,[5] G. L. Sun,[4] and D. L. Sun[4]

[1]*Institute for Superconducting and Electronic Materials, Faculty of Engineering, University of Wollongong, Wollongong, New South Wales 2522, Australia*
[2]*Department of Physics, Sabzevar Tarbiat Moallem University, P.O. Box 397, Sabzevar, Iran*
[3]*National Creative Research Initiative Center for Superconductivity, Department of Physics, Sogang University, Seoul 121-742, Republic of Korea*
[4]*Max Planck Institute for Solid State Research, Heisenbergstr 1, 70569 Stuttgart, Germany*
[5]*Department of Physics, University of Oslo, P.O. Box 1048, Blindern, 0316 Oslo, Norway*
[6]*CMSE, CSIRO, Lindfield, New South Wales 2070, Australia*
(Received 21 May 2010; published 28 July 2010)

We report that the (Ba,K)Fe$_2$As$_2$ crystal with $T_c = 32$ K shows a pinning potential, U_0, as high as 10^4 K, with U_0 showing very little field dependence. The (Ba,K)Fe$_2$As$_2$ single crystals become isotropic at low temperatures and high magnetic fields, resulting in a very rigid vortex lattice, even in fields very close to H$_{c2}$. The isotropic rigid vortices observed in the two-dimensional (2D) (Ba,K)Fe$_2$As$_2$ distinguish this compound from 2D high-T_c cuprate superconductors with 2D vortices. The vortex avalanches were also observed at low temperatures in the (Ba,K)Fe$_2$As$_2$ crystal. It is proposed that it is the K substitution that induces both almost isotropic superconductivity and the very strong intrinsic pinning in the (Ba,K)Fe$_2$As$_2$ crystal.

A high critical current density, J_c, upper critical field, B_{c2}, and irreversibility field, B_{irr}, a high superconducting transition temperature, T_c, strong magnetic-flux pinning, good grain connectivity, and isotropic superconductivity are the major physical requirements for superconducting materials used in practical applications operating at low and, in particular, high magnetic fields. The conventional low-T_c superconductors, where H_{c2} is also small, can only carry large J_c at very low temperatures. The cuprate high-T_c superconductors suffer from poor grain connectivity and easy melting of the vortex lattice, leading to small J_c in high magnetic fields at relatively high temperatures. For MgB$_2$ superconductor with T_c of 39 K, B_{irr} is far below H_{c2}, and J_c drops quickly with both field and temperature, preventing its use above 20 K. The newly discovered Fe-based superconductors[1–7] show T_c as high as 55 K and B_{c2} above 200 T, in combination with a small anisotropy for REFeAsO$_{1−x}$F$_x$ (RE-1111 phase, with RE a rare-earth element)[8] and an almost isotropic superconductivity for (Ba,K)Fe$_2$As$_2$ (122 phase).[9] These properties make the Fe-based superconductors extremely promising candidates for high magnetic field applications at relatively high temperatures. The current carrying ability of these superconductors at high fields and temperatures is largely determined by the flux-pinning strength and the behavior of the vortex matter. Therefore, the determination of their intrinsic vortex pinning strength is a central issue from both an applied and a fundamental perspective. Both 1111 and 122 phase compounds have typical two-dimensional (2D) crystal structures. In RE-1111 phase, where RE is a rare-earth element, the FeAs superconducting layers are separated by insulating LaO layers[10] while in Ba(K)-122 phase, the FeAs layer is sandwiched between conductive Ba layers.[5] It is expected that the 122 phase containing two FeAs layers would have small anisotropy and thus higher intrinsic pinning com-

pared to the single layer 1111 phase. Co-doped BaFe$_2$As$_2$ single crystal shows an anisotropy of 1–3 and upper critical-field values of $B_{c2}(B\|ab) = 20$ T and $B_{c2}(B\|c) = 10$ T at 20 K, with $dB_{c2}/dT \approx 5$ T/K.[11] For single crystals of the optimally doped Ba(Fe$_{1−x}$Co$_x$)$_2$As$_2$ with $x = 0.074$ and critical temperature $T_c \approx 23$ K, the anisotropy of the upper critical field, $\gamma = B_{c2}^{ab}/B_{c2}^c$, is in the range of 2.1–2.6, and the critical current density, J_c, is over 10^5 A/cm^2 and 3×10^5 A/cm^2 at 5 K for $B\|ab$ and $B\|c$, respectively.[11] The B_{c2} of (Ba$_{0.55}$K$_{0.45}$)Fe$_2$As$_2$ measured under pulsed magnetic fields exceeds 60 T at 14 K.[9] The anisotropy of B_{c2} is moderate (~3.5 close to T_c), and it drops with decreasing temperature, becoming isotropic at low temperatures.[9] Underdoped BaFe$_2$As$_2$ with T_c of 25 K shows an anisotropy of 3–4.[12]

Another important issue for practical applications is the occurrence of magnetic-flux jumps, which generally occur in larger samples with high critical current densities. Magnetic-flux jumps have been observed in thin-film forms of some type II superconductors, such as Nb$_3$Sn (Ref. 13) and MgB$_2$.[14] However, flux jumps have not yet been reported in any Fe-based superconductors so far.

In this paper, we report that the vortex lattice in (Ba,K)Fe$_2$As$_2$ crystals appears to be quite rigid, with pinning potentials as high as 10^4 K which show only weak-field dependences up to 10 T. The rigid three-dimensional (3D) vortex lattice in the two-dimensional (Ba,K)Fe$_2$As$_2$ seems to differ from the two-dimensional high-T_c cuprate superconductors with their more 2D pancakelike vortex lattices. Flux jumps were observed in one of our large samples at low temperature. The very strong intrinsic supercurrent carrying ability and flux pinning observed in the (Ba,K)Fe$_2$As$_2$ superconducting single crystals make this compound very promising for future applications in high magnetic fields.

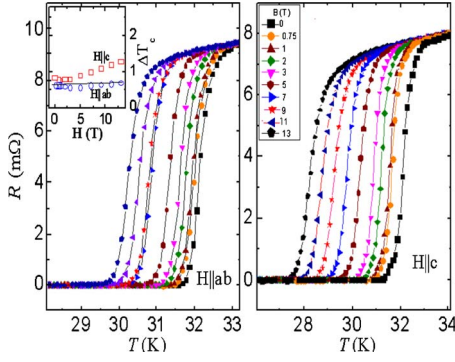The 122 crystals used in the present work was grown

FIG. 1. (Color online) Temperature dependence of the resistance of a $Ba_{0.72}K_{0.28}Fe_2As_2$ crystal measured for $H\|ab$ and $H\|c$ in different magnetic fields, $0 \leq H \leq 13$ T. Inset in the left panel shows the transition width as a function of magnetic field for both directions of applied field.

using a flux method. High purity elemental Ba, K, Fe, As, and Sn were mixed in a mol ratio of $(Ba_{1-x}K_xFe_2As_2):Sn = 1:45-50$ for the self-flux. A crucible with a lid was used to minimize the evaporation loss of K as well as that of As during growth. The crucible was sealed in a quartz ampoule filled with Ar and loaded into a box furnace. The details of the crystal growth are given in Ref. 15.

The electrical resistance R versus temperature curves of a $Ba_{0.72}K_{0.28}Fe_2As_2$ crystal for magnetic fields up to 13 T, applied parallel to the *ab* plane and to the *c* axis, are shown in Fig. 1. The resistance starts to drop toward zero at $T = 31.7$ K in zero magnetic field, indicating that the crystal is not optimally doped.[16] It can be seen that the onset of T_c decreases with increasing magnetic field very similar to $T_c(R=0)$, such that the transition width ΔT_c remains almost constant for both $B\|ab$ and $B\|c$ [see the inset in Fig. 1(a)]. When the field changes from 0 up to 13 T, the shape of $R(T)$ changes very little. This behavior is reminiscent of the magnetotransport behavior of conventional low-T_c superconductors and significantly different from that of cuprate high-T_c superconductors. In cuprate high-T_c superconductors, the T_c onset temperature does not change much but the $T_c(R=0)$ shifts to low temperature very quickly with field. The field-independent transition width ΔT_c is also quite different from what is observed in $NdFeAs_{0.2}OF_{0.8}$ single crystals, which show a broadening of $T_c(R=0)$ as the field increases.[8] In the following we define the temperature-dependent upper critical field $B_{c2}(T)$ by $R(T,B_{c2})=0.9R_n$, where R_n is the normal-state resistance just above the onset of T_c. In a similar way we define the irreversibility field $B_{irr}(T)$ by $R(T,B_{irr}) = 0.1 R_n$. The B_{c2} and B_{irr} obtained for both $B\|ab$ and $B\|c$ are denoted as B_{c2}^{ab}, B_{c2}^{c}, B_{irr}^{ab}, and B_{irr}^{c}, respectively.

It can be seen from Fig. 2 that the B_{c2} values for the $(BaK)Fe_2As_2$ are quite large ($B_{c2}^{ab}=13$ T at 30.7 K and $B_{c2}^{c} = 13$ T at 29 K). The slope dB_{c2}/dT is -7.5 and -4.4 for the *ab* and the *c* directions, respectively, for our $Ba_{0.72}K_{0.28}Fe_2As_2$ crystal. From Fig. 2, one can see that B_{irr} is very close to B_{c2} in both field directions, indicating that flux lattice melting in our the $(Ba,K)Ba_2As_2$ crystals seems to occur only over a relatively small area of the *B-T* phase diagram.

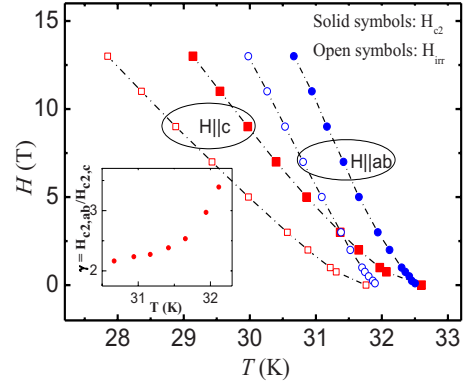FIG. 2. (Color online) H_{c2} and H_{irr} for both $H\|ab$ and $H\|c$ as a function of temperature. Inset: the anisotropy γ (H_{c2}^{ab}/H_{c2}^{c}) as a function of temperature.

The $B_{c2}(0)$ was estimated by using the Werthamer-Helfand-Hohenberg formula,[17] i.e., $B_{c2}(0)=-0.69 T_c(dB_{c2}/dT)$, with dB_{c2}/dT at $T=T_c$. We find $B_{c2}^{ab}(0) = 170$ T and $B_{c2}^{c}(0)=100$ T for our $(Ba,K)Fe_2As_2$ crystal. Furthermore, one can estimate $B_{c2}(0)$ from $B_{c2}(T) = B_{c2}(0)(1-t^2)/(1+t^2)$, where $t=T/T_c$ which results from the Ginzburg-Landau theory. One finds $B_{c2}^{ab}(0)=195$ T and $H_{c2}^{c}(0)=110$ T. The anisotropy $\gamma=B_{c2}^{ab}/B_{c2}^{c}$ of the 122 crystal was determined to be 2–3.5 for $T>30.5$ K, as can be seen in the inset of Fig. 2. The observed increase in γ with temperature T is opposite to that of Sm-1111 (Ref. 18) and MgB_2 (Ref. 19) superconductors, which might be due to multiband effects in 122 crystals.

According to the thermally activated flux flow model, the temperature and field dependence of the resistivity $R(T,B)$ is described by the equation $R(T,B)=R_0 \exp[-U(T,B)/k_BT]$, where R_0 is a parameter, k_B the Boltzmann's constant, and $U(T,B)$ is the activation energy for vortex bundle hopping, and we assume here $U(T,B)=U_0(B)(1-t)$. In the following we call U_0 the pinning potential. This pinning potential can be obtained from the slope of an Arrhenius plot, $\ln R(T,B)$ versus $1/T$. In Fig. 3, we have plotted the data as $\ln R$ vs $1/T$. The best fit to the experimental data yields values for the pinning potentials of $U_0=9100$ and 5900 K for $B\|ab$ and $B\|c$, respectively, at the low field of 0.1 T. These values are much higher than the reported values of $U_0 = 2000-3000$ K for $NdO_{0.82}F_{0.18}FeAs$ single crystals.[8] For comparison, we also include U_0 values for Bi-2212 (Ref. 20)
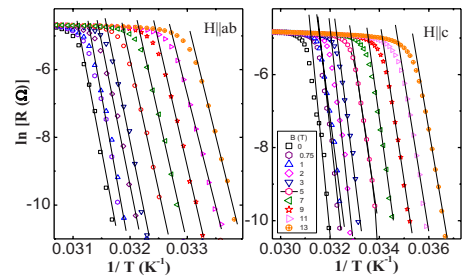

FIG. 3. (Color online) Natural logarithm of the resistance versus $1/T$ for field parallel (left) and perpendicular (right) to the *ab* direction.
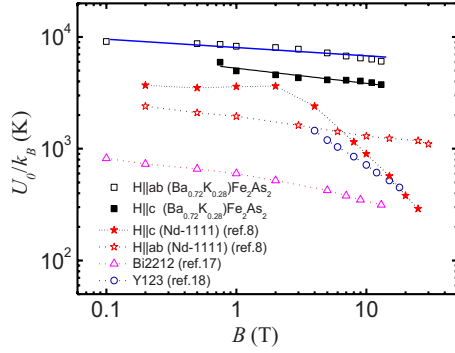
FIG. 4. (Color online) Field dependence of $U_0(B)$ for $Ba_{0.72}K_{0.28}Fe_2As_2$ crystal $(BaK)Fe_2As_2$.

and Y-123 (Ref. 21) single crystals in Fig. 4, even though their T_c's are different.

It has been reported that the pinning potential of bismuth strontium calcium copper oxide (BSCCO) crystals exhibits a power-law dependence on magnetic field, $U_0(B) \propto B^{-n}$, with $n=1/2$ for $B<5$ T and $n=1/6$ for $B>5$ T for $B\|c$.[20,22] However, for the $(BaK)Fe_2As_2$ crystal, U_0 drops very slowly with field as $B^{-0.09}$ and $B^{-0.13}$ for $B\|ab$ and $B\|c$, respectively (Fig. 4). This means that U_0 is almost field independent, which is a remarkable result. The values of U_0 for $(Ba,K)Fe_2As_2$ are three to four times larger than that of Bi-2212 (Ref. 21) and about ten times larger than that of Bi-2223 (Ref. 17) crystals. These values are also more than three times larger than those for $NdO_{0.82}F_{0.18}FeAs$ crystals.[8] Also, the U_0 for our $(Ba,K)Ba_2As_2$ crystal is about one order of magnitude higher than that of Y-123 crystals for fields above 1 T.[18] Thus the value of $U_0(B)$ of our $(Ba,K)Fe_2As_2$ single crystal is of record high compared to any other superconductor in single-crystal form.

It should be noted that the pinning potential of the $(BaK)Fe_2As_2$ crystal is almost field independent for the field range we have measured from 0 up to 13.5 T. However, it is expected that the U_0 should behave differently with field for higher fields, in particularly, for fields close to H_{c2}. Further study on the U_0 for the doped $BaFe_2As_2$ in higher fields is necessary.

A small $(Ba,K)Fe_2As_2$ single crystal in the shape of a long thin strip, obtained by cleaving along the ab plane, was investigated using magneto-optical imaging. The left inset in Fig. 5 is a magneto-optical image of the flux penetration into the sample, which was collected while applying a perpendicular field of 50 mT at 20 K. It is evident that the sample is of high uniformity, i.e., without any microcracks or weak links perturbing the flow pattern of the shielding current. Such regular flux patterns allow precise measurements of the critical current density J_c using the Bean critical state model formula for partial penetration in long thin strip geometry[23]

$$\cosh(\pi H/J_c d) = w/(w-2a),$$

where a is the advancement of the flux front into the strip at an applied field H, and w and d are the width and thickness of the strip, respectively. The obtained values for J_c in the
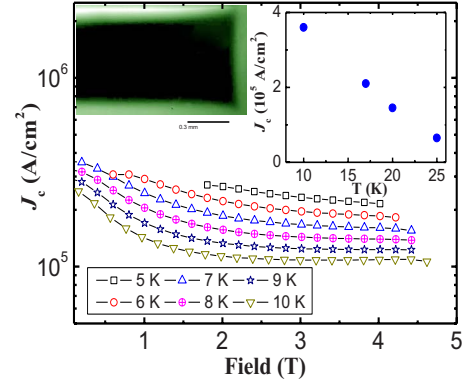

FIG. 5. (Color online) The J_c-field dependence obtained from the M-H loops (Fig. 6) measured on a large $Ba_{0.72}K_{0.28}Fe_2As_2$ crystal. Left inset: magneto-optical image of the flux penetration into the right half of the crystal. Right inset: critical current density versus temperature of a small $(Ba,K)Fe_2As_2$ single crystal shaped as a thin rectangular bar at $B=50$ mT.

temperature range 10–25 K are plotted in the right inset of Fig. 5.

Magnetization loops (Fig. 6) were collected for a relatively large $(Ba,K)Fe_2As_2$ single crystal $(4.2 \times 2.85 \times 0.15 \text{ mm}^3)$ at different fields $B\|c$ and temperatures down to 5 K. The J_c was obtained from the width ΔM of the magnetization loop using the Bean model, where for full sample penetration

$$J_c = 20\Delta\widetilde{M}w(1-\widetilde{w}3l).$$

Here l is the length of the sample. The resulting J_c versus applied field is plotted in Fig. 5.

For $B<4.5$ T and $T<10$ K the J_c is larger than 10^5 A/cm^2. The slow decrease in J_c with increasing field seems to correlate with the weak-field dependence of the pinning potential U_0. At 5 K, the J_c value is 2.7×10^5 A/cm^2 at $B=2$ T, and it only decreases to 2.2×10^5 A/cm^2 at $B=4$ T. The weak dependence of J_c on magnetic field and temperature suggests that the $(Ba,K)Fe_2As_2$ single-crystal superconductor has a superior
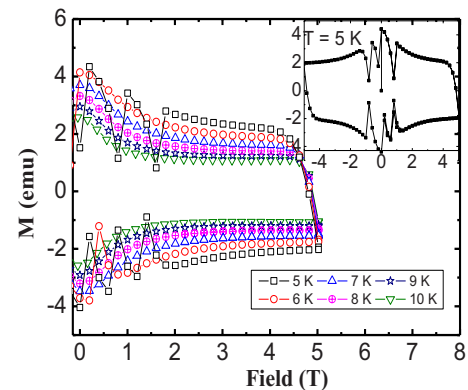

FIG. 6. (Color online) Magnetic hysteresis of a large $Ba_{0.72}K_{0.28}Fe_2As_2$ crystal. Inset shows a full loop at 5 K.
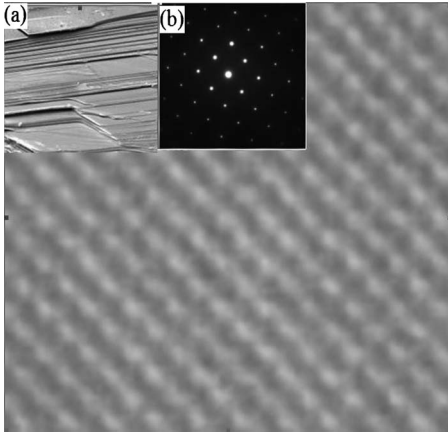
FIG. 7. High-resolution TEM image of a $Ba_{0.72}K_{0.28}Fe_2As_2$ crystal. The insets contain (a) a SEM image of the crystal surface and (b) an electron-diffraction pattern along the (001) direction.

J_c behavior, which is beneficial for potential applications in high magnetic fields.

In general, flux jumps can be observed in magnetization loop measurements of type II superconductors if the following criteria are fulfilled: (a) the sample is sufficiently large, (b) the J_c is sufficiently high, (c) the sample specific heat is small, and (d) the ramp rate of the magnetic field is sufficiently fast. As shown in Fig. 6, we have observed flux jumps in our large $(Ba,K)Fe_2As_2$ single crystals at temperatures below 7 K. The shapes of these magnetization jumps are very similar to the ones that have previously been observed and modeled in melt-textured YBCO samples.[24] So far, the occurrence of flux jumps has not been reported in any of the Fe-based superconductors.

Scanning electron microscopy (SEM) revealed that the 122 crystal has a typical 2D crystal structure [inset (a) in Fig. 7]. According to our transmission electron microscopy examination, we did not observe any noticeable crystal defects which could be possible pinning centers for the vortices. One of the typical atomic images taken along the [001] direction is presented in Fig. 7, which shows the typical features of square lattices on the (110) plane. All the surface atoms are perfectly ordered, and no superstructures are observed, as indicated by the selected large area electron-diffraction pattern [inset (b) in Fig. 7]. These results reveal that the 122 crystal has a very high crystallinity. Usually, the pinning is weak in a superconducting crystal with very high crystallinity. Here the question arises where the strong pinning comes from in a perfect 122 crystal. There are two possible causes one might think of. First, the K doping turns the parent compound from being nonsuperconducting into superconducting and at the same time introduces imperfections into the crystal lattice due to its different ionic size compared to Ba^{2+}. These lattice imperfections may act as intrinsic pinning centers in the $(Ba,K)Fe_2As_2$. Second, it has been reported that for the Fe-based superconductors, superconducting gaps vary with

the characteristic length scales of the deviations from the average gap value.[25] These variations in the gap magnitude, the zero-bias conductance, and the coherence peak strength are quite well matched to each other. Moreover, these are further correlated with the average separation between the K dopant ions in the superconducting FeAs planes for the $(Ba,K)Fe_2As_2$ crystal, which implies that the strength of the superconductivity is not uniform throughout the FeAs planes. The inhomogeneous superconducting strength may act as a source of pinning centers once magnetic flux exists inside the superconductor.

The nearly isotropic superconductivity[9] as indicated in the inset of Fig. 2, correlates well with the observed large critical current densities and large U_0 values in our $(Ba,K)Fe_2As_2$ single crystals. In $NdO_{0.82}F_{0.18}FeAs$ the pinning potential was found to be smaller, $U_0 = 2000–3000$ K.[8] This might be understood in terms of the stronger superconducting coupling between the FeAs superconducting layers in the FeAs-122 phase compared to the FeAs-1111 phase. In the FeAs-122 phase, there are two superconducting FeAs layers, and the coupling between the superconducting layers is stronger than in the FeAs-1111 phase, which results in nearly isotropic superconductivity as well as in a more 3D vortex lattice. That is to say, despite of the two-dimensional nature of crystal structure of the 122 phase, the vortex lattice can still be easily pinned by any pinning centers. Thus $(Ba,K)Fe_2As_2$ single crystals have the ability to carry large supercurrents in high magnetic fields. The 3D-like vortex lattice in $(Ba,K)Fe_2As_2$ single crystals distinguishes this compound from high-T_c cuprate superconductors such as BSCCO where layers of 2D pancake vortex lattices interact relatively weakly with each other.

In conclusion, we found that the $(Ba,K)Fe_2As_2$ crystal shows very high intrinsic flux-pinning strength, almost field independent high values of critical current density, high pinning potential of 10^4 K, high H_{c2}, high H_{irr}, and low values of anisotropy of 1–3. The obtained U_0 values are record high compared to any existing superconducting single crystal. The isotropic rigid vortices observed in the two-dimensional $(Ba,K)Fe_2As_2$ distinguish this compound from 2D high-T_c cuprate superconductors with 2D vortices. We observed the vortex avalanches in $(Ba,K)Fe_2As_2$ due to high J_c which further supports the high value of the pinning potential and the intrinsic strong flux pinning in this compound. It is the K substitution that induces both isotropic superconductivity and the very strong intrinsic pinning in the 122 compounds. The very strong intrinsic supercurrent carrying ability and flux pinning observed in the $(Ba,K)Fe_2As_2$ superconducting single crystals make this compound very promising for future applications in high magnetic fields.

*Author to whom correspondence should be addressed; xiaolin@uow.edu.au

†Deceased.

[1] Y. Kamihara, T. Watanabe, M. Hirano, and H. Hosono, J. Am. Chem. Soc. **130**, 3296 (2008).

[2] X. H. Chen, T. Wu, G. Wu, R. H. Liu, H. Chen, and D. F. Fang, Nature (London) **453**, 761 (2008).

[3] Z. A. Ren, J. Yang, W. Lu, W. Yi, X.-L. Shen, Z.-C. Li, G.-C. Che, X.-L. Dong, L.-L. Sun, F. Zhou, and Z.-X. Zhao, EPL **82**, 57002 (2008).

[4] C. Wang, L. Li, S. Chi, Z. Zhu, Z. Ren, Y. Li, Y. Wang, X. Lin, Y. Luo, S. Jiang, X. Xu, G. Cao, and Z. Xu, EPL **83**, 67006 (2008).

[5] M. Rotter, M. Tegel, and D. Johrendt, Phys. Rev. Lett. **101**, 107006 (2008); K. Sasmal, B. Lv, B. Lorenz, A. M. Guloy, F. Chen, Y.-Y. Xue, and C.-W. Chu, *ibid.* **101**, 107007 (2008).

[6] N. Ni, S. L. Bud'ko, A. Kreyssig, S. Nandi, G. E. Rustan, A. I. Goldman, S. Gupta, J. D. Corbett, A. Kracher, and P. C. Canfield, Phys. Rev. B **78**, 014507 (2008).

[7] X. L. Wang, S. R. Ghorbani, G. Peleckis, and S. Dou, Adv. Mater. **21**, 236 (2009).

[8] J. Jaroszynski, F. Hunte, L. Balicas, Y.-j. Jo, I. Raičević, A. Gurevich, D. C. Larbalestier, F. F. Balakirev, L. Fang, P. Cheng, Y. Jia, and H. H. Wen, Phys. Rev. B **78**, 174523 (2008).

[9] H. Q. Yuan, J. Singleton, F. F. Balakirev, S. A. Baily, G. F. Chen, J. L. Luo, and N. L. Wang, Nature (London) **457**, 565 (2009).

[10] F. Hunte, J. Jaroszynski, A. Gurevich, D. C. Larbalestier, R. Jin, A. S. Sefat, M. A. McGuire, B. C. Sales, D. K. Christen, and D. Mandrus, Nature (London) **453**, 903 (2008).

[11] N. Ni, M. E. Tillman, J.-Q. Yan, A. Kracher, S. T. Hannahs, S. L. Bud'ko, and P. C. Canfield, Phys. Rev. B **78**, 214515 (2008).

[12] H.-J. Kim, Y. Liu, Y. S. Oh, S. Khim, I. Kim, G. R. Stewart, and K. H. Kim, Phys. Rev. B **79**, 014514 (2009).

[13] I. A. Rudnev, S. V. Antonenko, D. V. Shantsev, T. H. Johansen, and A. E. Primenko, Cryogenics **43**, 663 (2003).

[14] T. H. Johansen, M. Baziljevich, D. V. Shantsev, P. E. Goa, Y. M. Galperin, W. N. Kang, H. J. Kim, E. M. Choi, M.-S. Kim, and S. I. Lee, Europhys. Lett. **59**, 599 (2002).

[15] G. L. Sun, D. L. Sun, M. Konuma, P. Popovich, A. Boris, J. B. Peng, K.-Y. Choi, P. Lemmens, and C. T. Lin, arXiv:0901.2728 (unpublished).

[16] H. Chen, Y. Ren, Y. Qiu, W. Bao, R. H. Liu, G. Wu, T. Wu, Y. L. Xie, X. F. Wang, Q. Huang, and X. H. Chen, EPL **85**, 17006 (2009).

[17] N. R. Werthamer, E. Helfant, and P. C. Hohenberg, Phys. Rev. **147**, 295 (1966).

[18] S. Weyeneth, R. Puzniak, U. Mosele, N. D. Zhigadlo, S. Katrych, Z. Bukowski, J. Karpinski, S. Kohout, J. Roos, and H. Keller, J. Supercond. Novel Magn. **22**, 325 (2009); L. Balicas *et al.*, arXiv:0809.4223 (unpublished).

[19] M. Angst, R. Puzniak, A. Wisniewski, J. Jun, S. M. Kazakov, J. Karpinski, J. Roos, and H. Keller, Phys. Rev. Lett. **88**, 167004 (2002); L. Lyard, P. Samuely, P. Szabo, T. Klein, C. Marcenat, L. Paulius, K. H. P. Kim, C. U. Jung, H.-S. Lee, B. Kang, S. Choi, S.-I. Lee, J. Marcus, S. Blanchard, A. G. M. Jansen, U. Welp, G. Karapetrov, and W. K. Kwok, Phys. Rev. B **66**,180502(R) (2002).

[20] T. T. M. Palstra, B. Batlogg, R. B. van Dover, L. F. Schneemeyer, and J. V. Waszczak, Phys. Rev. B **41**, 6621 (1990).

[21] D. López, L. Krusin-Elbaum, H. Safar, E. Righi, F. de la Cruz, S. Grigera, C. Feild, W. K. Kwok, L. Paulius, and G. W. Crabtree, Phys. Rev. Lett. **80**, 1070 (1998).

[22] X. L. Wang, A. H. Li, S. Yu, S. Ooi, K. Hirata, C. T. Lin, E. W. Collings, M. D. Sumption, M. Bhatia, S. Y. Ding, and S. X. Dou, J. Appl. Phys. **97**, 10B114 (2005).

[23] E. H. Brandt and M. Indenbom, Phys. Rev. B **48**, 12893 (1993).

[24] K.-H. Müller and C. Andrikidis, Phys. Rev. B **49**, 1294 (1994).

[25] Y. Yin, M. Zech, T. L. Williams, X. F. Wang, G. Wu, X. H. Chen, and J. E. Hoffman, Phys. Rev. Lett. **102**, 097002 (2009).